Influence of Arsenate Adsorption to Ferrihydrite, Goethite, and Boehmite on the Kinetics of Arsenate Reduction by Shewanella putrefaciens strain CN-32

ARTICLE *in* ENVIRONMENTAL SCIENCE & TECHNOLOGY · AUGUST 2011

Impact Factor: 5.33 · DOI: 10.1021/es201503g · Source: PubMed

6 AUTHORS, INCLUDING:

Jen-How Huang
University of Basel
41 PUBLICATIONS **528** CITATIONS
SEE PROFILE

Anna Lazzaro
ETH Zurich
28 PUBLICATIONS **221** CITATIONS
SEE PROFILE

Ruben Kretzschmar
ETH Zurich
233 PUBLICATIONS **7,032** CITATIONS
SEE PROFILE

Environmental Science & Technology

ARTICLE

pubs.acs.org/est

Influence of Arsenate Adsorption to Ferrihydrite, Goethite, and Boehmite on the Kinetics of Arsenate Reduction by *Shewanella putrefaciens* strain CN-32

Jen-How Huang,[†,*] Andreas Voegelin,[†,‡] Silvina A. Pombo,[†] Anna Lazzaro,[§] Josef Zeyer,[§] and Ruben Kretzschmar[†]

[†]Soil Chemistry Group, Institute of Biogeochemistry and Pollutant Dynamics, ETH Zurich, CHN, CH-8092 Zurich, Switzerland

[‡]Eawag, Swiss Federal Institute of Aquatic Science and Technology, Ueberlandstrasse 133, CH-8600 Duebendorf, Switzerland

[§]Environmental Microbiology Group, Institute of Biogeochemistry and Pollutant Dynamics, ETH Zurich, CH-8092 Zurich, Switzerland

Supporting Information

ABSTRACT: The kinetics of As(V) reduction by *Shewanella putrefaciens* strain CN-32 was investigated in suspensions of 0.2, 2, or 20 g L^{-1} ferrihydrite, goethite, or boehmite at low As (10 μM) and lactate (25 μM) concentrations. Experimental data were compared with model predictions based on independently determined sorption isotherms and rates of As(V) desorption, As(III) adsorption, and microbial reduction of dissolved As(V), respectively. The low lactate concentration was chosen to prevent significant Fe(III) reduction, but still allowing complete As(V) reduction. Reduction of dissolved As(V) followed first-order kinetics with a 3 h half-life of As(V). Addition of mineral sorbents resulted in pronounced decreases in reduction rates (32−1540 h As(V) half-life). The magnitude of this effect increased with increasing sorbent concentration and sorption capacity (goethite < boehmite < ferrihydrite). The model consistently underestimated the concentrations of dissolved As(V) and the rates of microbial As(V) reduction after addition of *S. putrefaciens* (~5 × 10^9 cells mL^{-1}), suggesting that attachment of *S. putrefaciens* cells to oxide mineral surfaces promoted As(V) desorption and thereby facilitated As(V) reduction. The interplay between As(V) sorption to mineral surfaces and bacterially induced desorption may thus be critical in controlling the kinetics of As reduction and release in reducing soils and sediments.

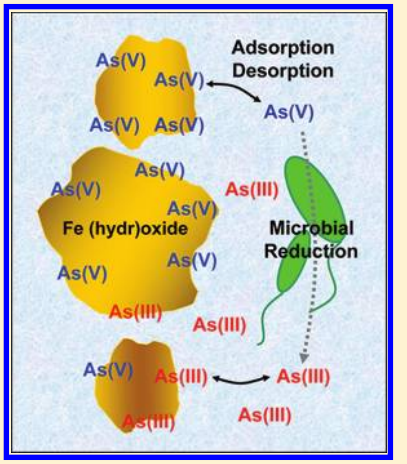

INTRODUCTION

Elevated concentrations of dissolved arsenic (As) in soil and groundwater cause serious health risks in many regions worldwide.[1,2] In most cases, elevated As concentrations are related to reducing (anoxic) conditions in flooded soils or aquifers.[3−5] Microbial reduction and dissolution of iron (Fe(III)) oxyhydroxides and/or reduction of sorbed arsenate (As(V)) are thought to be the driving factors for As release, which is under such conditions predominantly present in solution as arsenite (As(III)).[6−9] Iron oxyhydroxides are the most important sorbents for As(V) in most soils and aquifer sediments, although Al-hydroxides and edge-surfaces of clay minerals can also be important.[10−12] Reductive dissolution or transformation of poorly crystalline Fe(III)-oxyhydroxides into more crystalline solids can lead to a loss of sorption sites for As. Furthermore, under most natural conditions (e.g., dissolved concentrations <20 μM As), As(III) is less strongly sorbed to oxide and clay mineral surfaces than is As(V).[13−15]

The factors controlling the kinetics of microbial As reduction in the presence of Fe(III) oxyhydroxides are still poorly understood, including the interactions between As(V) and Fe(III) reduction and the role of As(V) desorption.[16] Most previous laboratory experiments on microbial As(V) reduction kinetics were conducted in the presence of rather high (i.e., millimolar range) lactate concentrations, which also led to substantial microbial Fe(III) reduction.[16,17] Resulting Fe mineral transformations, such as from ferrihydrite to magnetite, can counteract reductive As release in such model systems.[17−19] In many natural environments, however, microbial As(V) reduction proceeds under carbon-limited conditions, and As(V) may even be reduced without substantial Fe(III)-oxyhydroxide reduction.[4] Additionally, nonreducible sorbents such as Al-hydroxides or edge-surfaces of clay minerals may influence As(V) reduction kinetics in soils and sediments. It is therefore of great importance to understand the influence of adsorption of As(V) to oxide mineral surfaces on the kinetics of microbial As(V) reduction.

Some studies suggested that predominantly As(V) present in solution phase is reduced, rather than As(V) adsorbed to mineral surfaces. In a study with a detoxifying As(V) reducing bacteria *Clostridium* sp. strain CN-0, Jones et al.[20] found that the rate of microbial As(V) reduction in goethite suspensions was about 1200 times slower than for dissolved As(V). Therefore, processes responsible for the desorption of As(V) were suggested to

Received: May 2, 2011
Accepted: August 5, 2011
Revised: July 22, 2011
Published: August 05, 2011

dx.doi.org/10.1021/es201503g | *Environ. Sci. Technol.* 2011, 45, 7701–7709

control the reduction rate of As(V) to As(III). In another study with *Clostridium* sp. strain CN-8 at pH 6.8,[21] rapid reduction of dissolved As(V) but no reduction of As(V) sorbed to ferrihydrite was observed within 24 days. The authors concluded that desorption of As(V) was too slow to allow for detectable As(V) reduction. In other studies, direct reduction of adsorbed As(V) by bacteria was speculated to occur. Masscheleyn et al.[4] found in laboratory experiments with flooded soils that reduction and release of As occurred before detectable Fe(III) reduction. The authors explained their findings by As(V) reduction followed by As(III) desorption from Fe(III)-oxyhydroxides, in addition to reductive dissolution of the mineral phases under Fe(III) reducing conditions and consequent As release. Using X-ray adsorption near-edge structure (XANES) spectroscopy, Rochette et al.[22] demonstrated that As(V) in aluminum arsenate ($AlAsO_4 \cdot 2H_2O$) spiked into soil was rapidly reduced to As(III) during soil flooding but remained mostly bound in the solid phase. Irrespective of whether As(V) reduction proceeds exclusively in solution or involves also direct reduction of adsorbed As(V), surface interactions between As(V) and solid sorbent phases may strongly influence the rate of As(V) reduction. For the reduction of As(V) associated with solid phases in different ways by *Sulfurospirillum barnesii* at pH 7.3, Zobrist et al.[16] found that As(V) reduction rates decreased in the order: dissolved As(V) ≫ As(V) added to ferrihydrite shortly before microbial incubations > As(V) added to ferrihydrite 24 h before microbial incubations > As(V) coprecipitated with Fe(III) during ferrihydrite synthesis. The mode of As(V) association with ferrihydrite (e.g., surface adsorbed, coprecipitated) thus strongly affected As(V) reduction rates. The authors concluded that As(V) reduction kinetics were related to As(V) desorption rates and that sorbed As(V) was reduced much more slowly than dissolved As(V).

In these earlier studies, identification of the effect of As(V) adsorption to mineral surfaces on microbial As(III) reduction kinetics was confounded by two factors: (i) Experiments were often conducted at As surface loadings close to the sorption maximum of mineral surfaces where dissolved concentrations may still be relatively high, and (ii) high concentrations of organic C allowed not only for As reduction but also for a substantial reduction of mineral Fe(III) and resulting changes in mineral structure and surface chemistry.

The objectives of the present study therefore were (i) to investigate the kinetics of microbial As(V) reduction by *Shewanella putrefaciens* strain CN-32 at low total As (10 μM) and lactate (25 μM) concentrations in the absence and presence of different oxide mineral sorbents (ferrihydrite, goethite, and boehmite) and (ii) to compare the experimental results with independent model predictions based on the hypothesis that As(V) reduction occurs only via As(V) desorption followed by reduction of dissolved As(V). *S. putrefaciens* is a facultative anaerobic bacterium (rod-shaped, Gram-negative) which is well-known for its ability to reduce various electron acceptors including oxygen, manganese, iron, arsenic, and others.

MATERIALS AND METHODS

Mineral Sorbents. Ferrihydrite ($Fe_5HO_8 \cdot 4H_2O$) was prepared by dropwise addition of 1 M NaOH to 500 mL of a stirred and solution of 0.2 M $FeCl_3$ until pH 7.0 was reached.[23] The suspension was centrifuged (30 min, 2100*g*, 20 °C) and washed free of excess salts with autoclaved, doubly deionized (DDI) water (>18 MΩcm) prepared with a Milli-Q system (Millipore, U.S.). The ferrihydrite was directly used for experiments without drying or freezing to prevent changes in particle aggregation and microporous structure.[24] Goethite (α-FeOOH) was synthesized by adding 180 mL 5.0 M NaOH to 100 mL 1.0 M $FeCl_3$ solution, diluting the resulting suspension to 2 L with deionized water, followed by aging in a closed polypropylene flask at 70 °C for 72 h. [23]After cooling to room temperature, the goethite suspension was centrifuged (30 min, 2100*g*, 20 °C) and repeatedly washed with DDI-water until free of excess salt. After freeze-drying, the goethite was stored at 4 °C until use. Ferric chloride instead of Fe(III) nitrate was used for the synthesis of ferrihydrite and goethite to avoid nitrate impurities that could serve as electron acceptor for microbial respiration. Boehmite (γ-AlOOH) was purchased and used as received (Catapal-B, Sasol, U.S.). The specific surface areas of goethite and boehmite were 18.1 $m^2\ g^{-1}$ and 308 $m^2\ g^{-1}$, respectively, based on multipoint N_2−BET measurements (Sorptomatic, Thermo Fisher Scientific, U.S.). The specific surface area of the ferrihydrite was determined in an earlier study as ∼300 $m^2\ g^{-1}$.[25]

Suspensions of goethite or boehmite for reduction experiments were sterilized by autoclaving (121 °C, 20 min; SteriLine, Zirbus technology, Germany). For the experiments with ferrihydrite, all beakers, bottles, serum bottles, and neutral salt solutions were separately autoclaved. Ferrihydrite was synthesized using the sterile solutions and glass containers and synthesis was carried out in a sterile bench (BHA-48, Faster, The Netherlands). X-ray diffraction analysis (Cu Kα-radiation; Bruker AXS D4 Endeavor, Karlsruhe, Germany) confirmed the phase identity of ferrihydrite (2-line), goethite, and boehmite and showed that autoclaving prior to incubation had no detectable effect on the structure or crystallinity of goethite and boehmite.

Desorption and Adsorption of As(V) and As(III). The kinetics of desorption of As(V) and adsorption of As(III), respectively, and adsorption equilibria (isotherms) of both species were studied in batch experiments in the absence of bacteria, but using the same solution composition as for microbial reduction experiments (pH 7, 10 mM PIPES, (piperazine-*N*,*N*′-bis-(2-ethanesulfonic acid)), 5 mM NaCl, 25 μM sodium lactate, 0.5 mM $CaCl_2$ and $MgCl_2$). For these experiments, solids concentrations of 0.02 g L^{-1} ferrihydrite, 1 g L^{-1} goethite, and 0.2 g L^{-1} boehmite were used to ensure that dissolved As concentrations after equilibration were sufficiently high for their accurate determination by ICP-MS.

For measuring As(V) desorption kinetics, the mineral suspensions were pre-equilibrated for 24 h with 1 to 10 μM As(V). Desorption was then induced by replacing 90% of the solution phase with As(V)-free solutions of identical composition after centrifugation. We chose to replace 90% of the solutions in all experiments to avoid accidental loss of solid particles. As(V) desorption was thereafter followed over time by analyzing for dissolved As(V). The As(III) adsorption kinetics for all three sorbents were studied by adding 2−8 μM As(III) to metal oxide suspensions under constant stirring. Subsamples of the suspension were extracted with a syringe at different time intervals, immediately passed through 0.2 μm filter membranes (cellulose acetate), and analyzed for total As.

Adsorption isotherms of As(III) and As(V) were determined for all three sorbents covering large concentration ranges (0.1 to 50 μM As(V) and 0.1 to 25 μM As(III)). The suspensions were equilibrated for 24 and 2 h for As(V) and As(III), respectively. The equilibration time was kept shorter for As(III) to avoid oxidation of As(III) to As(V). Additional details on adsorption

and desorption experiments are provided in the Supporting Information (SI), and can also be found in Huang et al.[15] The sorption isotherm and kinetics data were used for the parametrization of our As(V) reduction kinetics model described below.

Microbial As(V) Reduction Experiments. *Shewanella putrefaciens* strain CN-32, obtained as ATCC BAA-1097, was grown for 24 h to late-exponential phase under oxic conditions in tryptic soy broth at 30 °C. Cell densities of each culture were estimated from optical density measurements at 600 nm (OD_{600}), which were calibrated against total cell numbers determined by counting of DAPI (4′,6-diamidino-2-phenylindol)-stained cells using an optical microscope (Leica Microsystems, Wetzlar, Germany). Cells were harvested by centrifugation (2100*g*, 15 min at 4 °C) and washed twice with a solution containing 10 mM PIPES buffer (pH 7.0) and neutral salts (5 mM NaCl; 0.5 mM $CaCl_2$; 0.5 mM $MgCl_2$). The washed cells were resuspended in 2 mL wash solution and kept at 4 °C for less than 3 h until inoculation.

The kinetics of microbial reduction of As(V) was studied in batch experiments using 50 mL serum bottles capped with butyl rubber septa and crimp-sealings. All experiments were carried out in 10 mM PIPES buffer adjusted to pH 7.0 and at constant background electrolyte concentrations (5.0 mM NaCl; 0.5 mM $CaCl_2$; 0.5 mM $MgCl_2$). As(V) and lactate were added from filter-sterilized solutions (0.2 μm, cellulose acetate, FP 30/0,2 CA-S, Whatman). Initially, all solutions or suspensions contained 1 to 10 μM As(V), 25 μM Na-lactate, and $\sim 5 \times 10^9$ cells mL^{-1}. First, the As(V) solutions or suspensions containing the sorbent minerals and all solutes were prepared in 8 mL volume, to be diluted to the final volume of 10 mL by addition of 2 mL cell suspension to start the reduction experiments. After addition of cells, the serum bottles were repeatedly evacuated and purged with N_2-gas for 10 min to remove all oxygen. The bottles were then incubated on a rotary shaker (250 rpm) at 25 °C. During the incubation period, 1 mL aliquots were periodically withdrawn from the suspensions under N_2-atmosphere using a syringe. The samples were immediately analyzed for As(V) and As(III) after each sampling time to prevent changes in As speciation. The microbial reduction kinetics of dissolved As(V), that is, in the absence of mineral sorbents, were studied using solutions with initial As(V) concentrations of 1, 4, 7, and 10 μM. In the experiments with mineral solids the initial As(V) concentration was 10 μM and the solid concentrations were 0.2, 2, or 20 g L^{-1} of ferrihydrite, goethite, or boehmite. Before adding *S. putrefaciens* CN-32 cells, the suspensions were first equilibrated for 24 h and the initial distribution of As(V) between the solution and solid phases was determined.

Analysis of Total and Dissolved As(V) and As(III). A part of each sample was filtered through 0.2 μm membranes (Nylon, Wicom, Germany) for the analysis of dissolved As(V), As(III), Fe(total) and Fe(II). Another part of the samples was analyzed without filtration after dissolution of mineral sorbent particles to determine the total concentrations of As(V), As(III), and Fe(II). The concentrations of sorbed As(V), As(III), and Fe(II) were calculated from the differences between total and dissolved concentrations. The total dissolution of mineral sorbents was achieved in 4 M HCl + 10% acetic acid (HOAc) for 1 h at 95 °C for goethite and boehmite and at room temperature for ferrihydrite.[26] Under these strongly acidic extraction conditions and high HOAc and Cl^- concentrations, As(III) is effectively stabilized against oxidation by O_2.[26]

Speciation analysis of As(III) and As(V) was performed on a PRP-X100 anion-exchange column (4 × 20 mm; Hamilton Company, USA) at 22 °C with a mobile phase (1.0 mL min^{-1}) of 2 mM $(NH_4)H_2PO_4$ adjusted to pH 6.0 with NH_3. A high-performance liquid chromatography instrument (HPLC, Agilent 1200 series), consisting of a gradient pump, capillary PEEK tubing (0.25 mm i.d.), a 100 μL injection loop, and an autosampler was connected to the ion exchange column and coupled to an inductively coupled plasma mass spectrometer (ICP-MS; Agilent 7500ce, Japan). A multispecies working solution for calibration of As(III) and As(V) with a total concentration of 0, 10, 20, 40, 80, and 100 μg As L^{-1} was prepared before each use by diluting the stock solutions with PIPES buffered working solutions. Concentrations of total As were determined by ICP-MS, and the Fe(II) and Fe(III) concentrations of were quantified using a colorimetric 1,10-phenanthroline method with a detection limit of 2.5 μM for dissolved Fe(II) and Fe(III). Due to required sample dilution and absorbance interference by Fe(III), the detection limits for Fe(II) in the solid phases (after total dissolution) were higher: 0.1, 0.35, and 3.5 mM Fe(II) for suspensions with 0.2, 2, and 20 g kg^{-1} oxyhydroxides, respectively. Thus, this allowed detection of Fe(II) in the solid phases if more than 2−5% of the total Fe were reduced.

Prediction of As(V) Reduction Kinetics in the Presence of Mineral Sorbents. Independent model predictions of As(V) reduction kinetics in the presence of mineral sorbent phases were performed based on the hypothesis that only dissolved As(V) is reduced by *S. putrefaciens* CN-32. Other possible reduction pathways and possible bacteria-mineral interactions were neglected in these model calculations. Experimental data for microbial reduction kinetics of dissolved As(V) in the absence of sorbents, as well as adsorption equilibria (isotherms) of As(III) and As(V), desorption kinetics of As(V), and adsorption kinetics of As(III) to the mineral sorbents in the absence of bacteria were used to independently parametrize rate and adsorption coefficients.

Adsorption equilibria of As(III) and As(V) were obtained from the adsorption isotherms presented in Figure 1 and were described by fitting a two-site Langmuir isotherm equation:

$$S_{eq} = \frac{K_{L1} b_{max\ 1} C_{eq}}{1 + C_{eq}} + \frac{K_{L2} b_{max\ 2} C_{eq}}{1 + C_{eq}} \quad (1)$$

where S_{eq} (μmol g^{-1}) and C_{eq} (μmol L^{-1}) are the sorbed and corresponding dissolved concentrations of either As(V) or As(III) at equilibrium, K_{L1} and K_{L2} (L μmol^{-1}) the respective Langmuir sorption coefficients and b_{max1} and b_{max2} (μmol g^{-1}) the maximum adsorption capacities for either As(V) or As(III). In the case of As(III) sorption to boehmite, a one-site Langmuir equation (eq 1 with $b_{max2} = 0$) was sufficient to describe the data.

Desorption kinetics of As(V) and adsorption kinetics of As(III) were described using kinetic rate equations adapted from eq (11) and (12) in Yin et al.[27] Accordingly, the desorption kinetics of As(V) were described using the first-order rate expression:

$$\frac{dC_t}{dt} = k_{des}(C_{eq} - C_t) \quad (2)$$

where C refers to dissolved concentration of As(V) at equilibrium (eq) or time t (h), and k_{des} (h^{-1}) is the desorption rate coefficient for As(V). The adsorption kinetics of As(III) were described using the second-order rate expression:

$$\frac{dS_t}{dt} = k_{ads}(S_{eq} - S_t)C_t \quad (3)$$

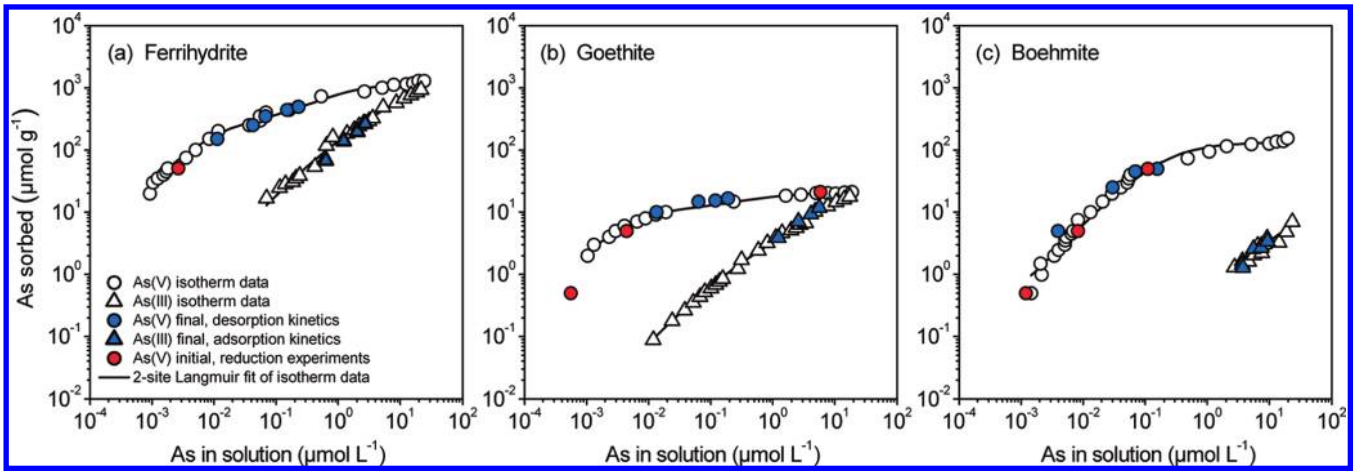

Figure 1. Adsorption isotherms for As(V) and As(III) on (a) ferrihydrite, (b) goethite, and (c) boehmite at 23 °C. For comparison, the final concentrations of dissolved As in experiments on adsorption (As(III)) and desorption (As(V)) kinetics (see SI Figures S2 and S3), and the initial As(V) concentrations in reduction experiments are shown. Lines represent two-site Langmuir isotherm fits of the adsorption data, which were used in model predictions of As(V) reduction kinetics. The legend in (a) applies for all panels. Experimental adsorption isotherm data in (a) and (b) were previously published by Huang et al.[15].

where S and C refer to sorbed and dissolved concentrations of As(III) at equilibrium or time t, and k_{ads} (μM^{-1} h^{-1}) is the adsorption rate coefficient. Both, k_{des} and k_{ads} were obtained by fitting the experimental data for As(V) desorption and As(III) adsorption kinetics for ferrihydrite, goethite, and boehmite using Origin 8.0 (OriginLab Corporation, U.S.). Detailed fit results are provided in the SI.

The reduction of dissolved As(V) to As(III) was described by a first-order rate equation:

$$\frac{dC_{As(V)}}{dt} = -k_{red}C_{As(V)} = \frac{-dC_{As(III)}}{dt} \quad (4)$$

where k_{red} (h^{-1}) is the rate coefficient of microbial reduction of dissolved As(V).

RESULTS

Arsenic Sorption in the Absence of Bacteria. Figure 1 shows equilibrium adsorption isotherms for As(V) and As(III) on ferrihydrite, goethite, and boehmite along with the respective 2-site Langmuir model fits. Note, that these isotherms cover more than 4 orders of magnitude in dissolved As(III) and As(V) concentrations, and that the concentration ranges are much lower than in most previously published studies. As(V) was generally sorbed more strongly than As(III). However, As(III) adsorption isotherms exhibited much steeper slopes than those of As(V), and the isotherms therefore converged at high dissolved As concentrations. Similar amounts of As(V) and As(III) were adsorbed on ferrihydrite and goethite when the dissolved As concentrations were around 20−30 μM. In contrast, As(III) sorption to boehmite was always much lower than sorption of As(V), even at high dissolved As concentrations. The maximum amounts of As sorbed per mass of sorbent decreased in the order ferrihydrite > boehmite > goethite. This can in part be explained by the large differences in specific surface area of the sorbent phases. The initial dissolved As concentrations in incubation experiments (i.e., after pre-equilibration and before adding bacteria) and the final concentrations in the kinetics experiments (SI, Figure S2) are also plotted in Figure 1 for comparison

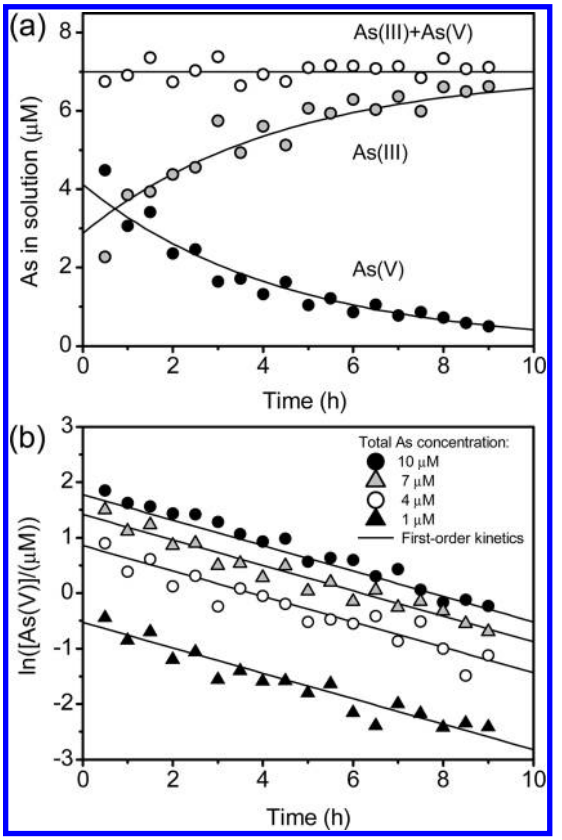

Figure 2. (a) Concentrations of dissolved As(V), As(III), and the sum of both species during reduction of 7 μM As(V) by *S. putrefaciens* strain CN-32 in the absence of mineral sorbents. (b) Natural logarithm of the concentrations of dissolved As(V) during reduction of 1, 4, 7, and 10 μM As(V) by *S. putrefaciens* in absence of mineral sorbents. Lines represent a first-order kinetics rate expression (eq 2) fitted simultaneously to all data. The resulting rate coefficient was k_{red} = 0.229 ± 0.008 (h^{-1}).

(closed symbols). All points are in good agreement with the adsorption isotherms, demonstrating that the same sorption equilibrium was always reached in these experiments. This is

very important for the subsequent model predictions of microbial As(V) reduction in the presence of sorbents, which was based on the fitted Langmuir isotherms, the adsorption and desorption rate coefficients of As(V) and As(III), and reduction kinetics of As(V) in solution, respectively.

Microbial Reduction of Dissolved As(V). The reduction kinetics of dissolved As(V) by *S. putrefaciens* CN-32 in the absence of mineral sorbents is presented in Figure 2. After inoculating with 5×10^9 cells mL^{-1} the solutions with initial (at $t = 0$) As(V) concentrations ranging from 1 to 10 μM, the As(V) concentration decreased and the As(III) concentration increased, respectively. Both concentrations were measured independently, and their sums were in good agreement with the respective total As concentrations, as shown for the experiment with 7 μM As in Figure 2a. The rate coefficients for As(V) reduction at different initial As(V) concentrations were determined by fitting a linear regression to ln-transformed, normalized concentrations, $\ln(C_t/C_0)$. This yielded a first-order rate coefficient of $0.229 \pm 0.008\ h^{-1}$, which accurately describes the kinetics of the reduction of dissolved As(V) by *S. putrefaciens* CN-32 over a concentration range of 1−10 μM As(V) (Figure 2b). This rate coefficient corresponds to an As(V) half-life ($t_{1/2}$) of 3.0 h.

Microbial Reduction of As(V) in the Presence of Sorbents. The kinetics of microbial As(V) reduction in the presence of different concentrations of ferrihydrite, goethite, and boehmite are shown in Figure 3 and first-order rate coefficients obtained from linear regression fits to the ln-transformed data for total As(V) normalized to its initial concentration are summarized in Table 1. In comparison to dissolved As(V) with $t_{1/2}$ = 3 h (dashed lines in Figure 3), half-lives of 32, 111, and 227 h were obtained for As(V) in suspensions of 0.2 g L^{-1} goethite, boehmite, and ferrihydrite, respectively, indicating a strong decrease in As(V) reduction rate with increasing extent of As(V) sorption. In agreement with this trend among different sorbents, also increasing solids concentrations caused a marked decrease in As(V) reduction rate coefficients and corresponding increases in As(V) half-life (Table 1). In the presence of 2 and 20 g L^{-1} ferrihydrite, As(V) reduction was not detectable within 100 h of incubation.

Figure 4 shows the concentrations of dissolved As(V) and As(III) during reduction experiments in suspensions with three different goethite concentrations. Corresponding data for the other sorbents are provided in the SI. The experimental data are compared with model predictions based on desorption kinetics of As(V), adsorption kinetics of As(III), sorption equilibria for As(V) and As(III), and reduction kinetics of As(V) in solution. At the lowest goethite concentration, the model predictions were reasonably close to the experimental data (Figure 4a). The initial dissolved As(V) concentration was highest and it decreased rapidly due to microbial reduction of As(V). Concurrently, the dissolved concentration of As(III) increased as was predicted by the model. However, increasing the goethite concentration to 2 or 20 g L^{-1} led to strong discrepancies between experimental results and model predictions. The initial dissolved As(V) concentrations decreased strongly with increasing goethite concentrations (note the different scale in Figure 4c), and consequently, the microbial As(V) reduction rates and release of As(III) to solution were much lower. Dissolved As(V) concentrations in the suspension with 20 g L^{-1} goethite increased over time, which was not adequately predicted by the model. Similar results were obtained for the other sorbents. Overall, the model consistently underestimated the rates of microbial As(V) reduction in the presence of mineral sorbents.

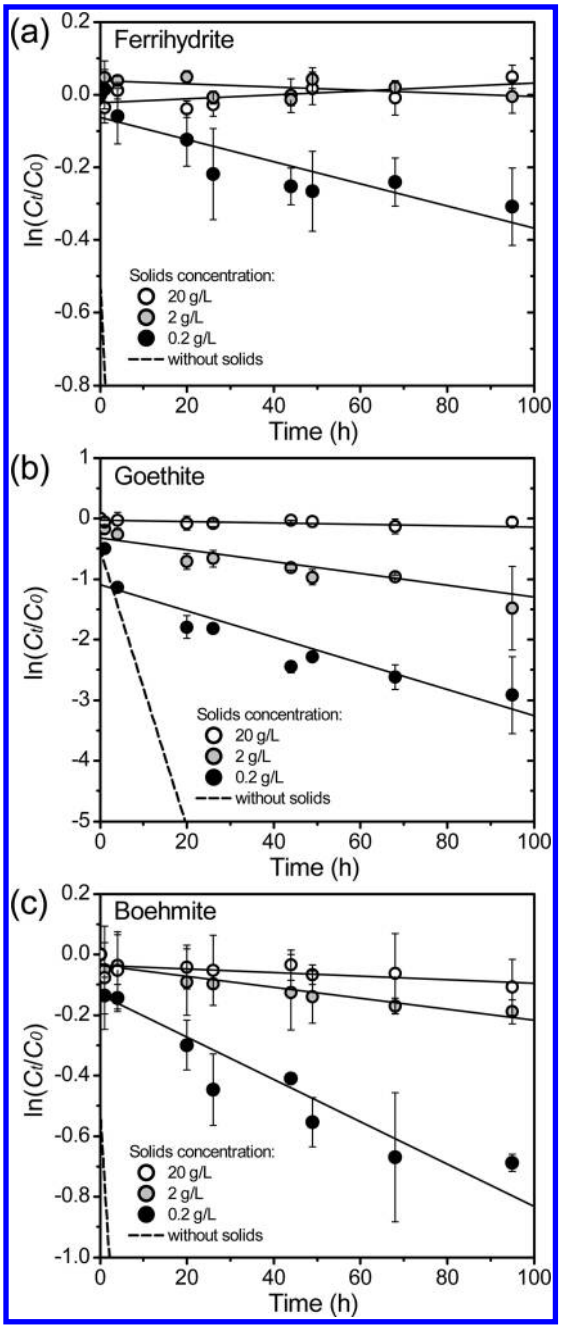

Figure 3. Kinetics of As(V) reduction by *S. putrefaciens* strain CN-32 in the presence of (a) ferrihydrite, (b) goethite, and (c) boehmite. The data are plotted as natural logarithm of total (solid and solution phase) As(V) concentrations (C_t) normalized to the initial As concentration C_0. Error bars represent the standard deviations of three replicates and solid lines are linear regression fits to the data, yielding first-order rate coefficients (Table 1). Dashed lines show the kinetics of As(V) reduction in the absence of mineral sorbents (from Figure 2) for comparison.

DISCUSSION

Influence of Adsorption on the Kinetics of Microbial As(V) Reduction. Our results clearly demonstrate that the presence of mineral sorbents strongly retards microbial As(V) reduction by *S. putrefaciens* CN-32, indicating that reduction of adsorbed As(V) is insignificant or at least much slower than that of dissolved As(V). On a mass unit basis, the relative effects exerted

Table 1. First-Order Rate Coefficients (k_{red}) and Corresponding Half-Lives ($t_{1/2}$) for Reduction of 10 μM Total Initial As(V) by *S. putrefaciens* strain CN-32 in the Absence and Presence of Ferrihydrite, Goethite, or Boehmite as Mineral Sorbents[a]

sorbent mineral	solids concentration (g L^{-1})	solids surface area (m^2 L^{-1})	experimental		predicted	
			k_{red} (h^{-1})	$t_{1/2}$ (h)	k_{red} (h^{-1})	$t_{1/2}$ (h)
no sorbent	0	0	2.29×10^{-1}	3		
ferrihydrite	0.2	60	3.05×10^{-3}	227	3.98×10^{-5}	17 400
ferrihydrite	2	600	4.49×10^{-4}	1540	3.42×10^{-6}	203 000
ferrihydrite	20	6000	n.r.	n.r.	3.37×10^{-7}	2 050 000
goethite	0.2	3.6	2.16×10^{-2}	32	9.38×10^{-3}	74
goethite	2	36	9.75×10^{-3}	71	7.12×10^{-5}	9730
goethite	20	362	1.16×10^{-3}	597	4.40×10^{-6}	158 000
boehmite	0.2	62	6.24×10^{-3}	111	2.52×10^{-3}	275
boehmite	2	616	1.68×10^{-3}	413	1.77×10^{-4}	3910
boehmite	20	6160	5.85×10^{-4}	1190	1.72×10^{-5}	40 400

[a] Predicted values are based on the simplifying assumption that only dissolved As(V) is reduced by *S. putrefaciens*, ignoring possible bacteria-mineral interactions. The model was calibrated with independent adsorption isotherm and adsorption/desorption kinetics experiments. n.r. = no detectable As(V) reduction within 100 h.

by the different sorbents increased in the order goethite < boehmite < ferrihydrite, which can partly be explained by their differences in specific surface area and microporosity. Ferrihydrite has the largest specific surface area and a microporous structure leaving a considerable fraction of sorption sites inaccessible for direct contact with microorganisms. Correspondingly, addition of 2 g L^{-1} goethite led to a 96% decrease of the As(V) reduction rate, while addition of 20 g L^{-1} ferrihydrite completely suppressed As(V) reduction by *S. putrefaciens* CN-32 within 100 h (Table 1; Figure 3). Comparable effects of adsorption on As(V) reduction were previously observed by Zobrist et al.[16] using suspensions of ferrihydrite and *Sulfurospirillum barnesii* at 0.8−1 mM As(V) buffered with HEPES at pH 7.3.

In contrast to many previous studies, we added low concentrations of lactate (25 μM) to minimize the possible influence of Fe(III)-reduction on As mobilization and readsorption. This concentration was sufficient to reduce all of the 10 μM As(V) based on reaction stoichiometry ($lactate^- + 2\ HAsO_4^{2-} + 3H^+ \rightarrow acetate^- + 2\ H_3AsO_3^0 + HCO_3^-$), but would have allowed for the reduction of at most 5% of the total Fe(III) at the lowest suspension concentrations (0.2 g L^{-1}) of ferrihydrite or goethite if all lactate were used for Fe(III)-reduction. For the 2 and 20 g L^{-1} suspensions, the maximum percentages of Fe that could theoretically be reduced by 25 μM lactate would be 0.5% and 0.05%, respectively. Another process which could affect Fe(III)-oxyhydroxide dissolution is the production of Fe(III)-solubilizing organic ligands, as was shown for *S. putrefaciens* strain 200.[28] However, in our experiments we never detected dissolved Fe(II) or Fe(III) using the colorimetric 1,10-phenanthroline method, suggesting that microbial Fe(III)-reduction and Fe(III)-solubilization were indeed negligible and did not significantly alter the mineralogy or specific surface area of the solids. In a related experiment conducted under similar conditions, no transformation of ferrihydrite to other iron mineral phases could be detected by Fe K-edge EXAFS spectroscopy (data not shown). Our data on As(V) reduction kinetics in the presence of mineral sorbents showed apparent decreases in the reduction rate with time, especially at the lowest solid concentrations (0.2 g L^{-1}) (Figure 3). This was most likely caused by the decreasing dissolved As(V) concentrations in the initial phase of the incubations. The most remarkable case was the incubation at 0.2 g L^{-1} goethite in which As(V) reduction was as rapid as that of dissolved As(V) during the first 5 h (Figure 3b). Figure 4a shows that the As(V) concentration rapidly decreased during the first hours of incubation, explaining this decrease in reduction rate.

Langner and Inskeep[21] concluded from their studies that As(V) desorption was too slow to cause significant increases in dissolved As concentration during As(V) reduction by *Clostridium* sp., strain CN8. However, our experiments on As(V) desorption kinetics showed that the equilibrium concentrations of dissolved As(V) were typically reached within less than 15 min, which is rather fast compared to the half-life of As(V) during microbial reduction of dissolved As(V) ($t_{1/2}$ = 3 h). This suggests that in our experiments the overall As(V) reduction rate in the presence of mineral sorbents was limited by the low equilibrium concentration of As(V) in solution rather than by slow As(V) desorption kinetics, as postulated by Langner and Inskeep.[21] From our results, we hypothesize that the reduction of As(V) in the presence of mineral sorbents by *S. putrefaciens* CN-32 proceeds predominantly via As(V) desorption and subsequent reduction of dissolved As(V). This was the basis for the model simulations discussed in the following section.

Experimental versus Predicted As(V) Reduction Rates. Based on the hypothesis that microbial As(V) reduction by *S. putrefaciens* CN-32 in the presence of mineral sorbents occurs only via As(V) desorption and subsequent microbial reduction of dissolved As(V), we performed model predictions as described earlier. Experimental and predicted first-order rate coefficients for microbial As(V) reduction in the absence and presence of sorbents and corresponding half-lives for As(V) are reported in Table 1. The kinetic model consistently underestimated the rates of microbial As(V) reduction in the presence of mineral sorbents, whereby the discrepancy between experimental and predicted As(V) reduction increased with increasing sorbent concentration (Figure 4). For example, the predicted As(V) reduction rates were 2.3, 136, and 265 times lower than the corresponding experimental rates in the presence of 0.2, 2, and 20 g L^{-1} goethite, respectively (Table 1).

The increasing discrepancies between observed and predicted As(V) reduction rates with increasing sorbent concentrations suggest that additional factors influence microbial As(V) reduction in the presence of sorbents. Some possible processes that have to be considered include: (i) additional reduction of adsorbed As(V) by *S. putrefaciens* CN-32, and subsequent partial

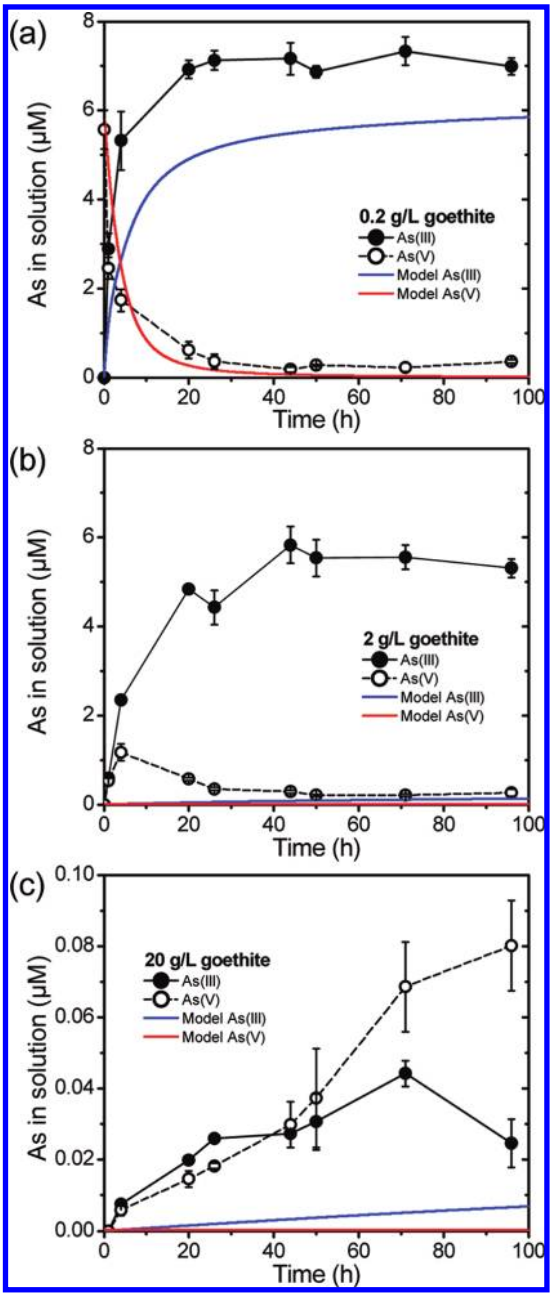

Figure 4. Concentrations of dissolved As(V) and As(III) during As(V) reduction by *S. putrefaciens* strain CN-32 in the presence of (a) 0.2 g/L, (b) 2 g/L, and (c) 20 g/L goethite. Error bars represent the standard deviations of three replicates. Experimental data are compared with corresponding model predictions based on the simplifying assumption that only dissolved As(V) is reduced, ignoring possible bacteria-mineral interactions. The model was calibrated with independent adsorption isotherm and adsorption/desorption kinetics experiments.

desorption of As(III), (ii) additional abiotic reduction of As(V) by Fe(II) resulting from small amounts of Fe(III)-reduction, (iii) additional bacteria-induced desorption of As(V), with subsequent microbial reduction of dissolved As(V). These possible contributions are discussed in the following.

To date, it is still unclear whether bacteria directly reduce adsorbed As(V), although it is well established that bacteria use different strategies to reduce sparingly soluble Fe(III)-oxyhydroxides, for example, direct contact,[29] producing nanowires,[30] or secreting organic electron-shuttling compounds (e.g., *Shewanella* species [31]). However, in our experiments with 2 and 20 g L^{-1} ferrihydrite, the initial concentrations of dissolved As(V) were below the detection limit of the ICP-MS (0.13 nM), and no As(V) reduction was observed. This suggested that direct reduction of adsorbed As(V) was much less important than reduction of dissolved As(V) during our short-term incubations. The second possible process, abiotic reduction of As(V) by Fe(II), seems very unlikely considering recent reports in the literature: In an abiotic control experiment, Zobrist et al.[16] checked for possible As(V) reduction in the presence of Fe(II) in ferrihydrite suspensions containing HEPES buffer (7.5 mM; pH 7.3), but detected no As(III) in solution or sorbed to the solid phase. Similarly, Amstaetter et al.[32] observed no reduction of As(V) under strictly anoxic conditions by "Fe(II)-activated" goethite, that is, goethite with adsorbed Fe(II). Surprisingly, the authors did observe oxidation of As(III) to As(V) by Fe(II)-activated goethite under anoxic conditions, suggesting that Fe(II) on the goethite surface formed a highly reactive, As(III)-oxidizing surface site of unknown nature. Based on these two studies, we can exclude abiotic As(V) reduction by trace amounts of Fe(II) in our experiments with ferrihydrite and goethite. Moreover, this mechanism would not apply to the boehmite suspensions, for which the discrepancies between observed and predicted rate coefficients were of similar magnitude.

The third possible process, enhanced As(V) reduction as a result of bacteria-induced As(V) desorption from the solid phases, may have played a very significant role. Before the addition of bacterial cells, the concentrations of dissolved As(V) in the incubation experiments were consistent with the adsorption isotherms determined in the absence of bacteria (Figure 1). However, substantially higher As(V) concentrations than expected from the adsorption isotherms were recorded after *S. putrefaciens* CN-32 cells were added and the suspensions were incubated for 100 h. In the model calculations, this discrepancy was reflected in much higher experimental than predicted concentrations of dissolved As(V) (Figure 4). Similarly, almost all concentrations of dissolved As(III) in the incubation experiments strongly deviated from the isotherms, likely reflecting the desorptive effect of *S. putrefaciens* CN-32 cells.

Indirect effects of bacteria on As(V) adsorption equilibria due to changes in solution composition can be excluded, because buffering with 10 mM PIPES has successfully kept the pH stable at 7.0 during incubation and the effects of both lactate and acetate on As(V) adsorption were negligible (SI, Figure S1). Also, As(III) formed during microbial As(V)-reduction cannot effectively compete with As(V)-adsorption in the concentration range used in this study (Figure 1). Therefore, the decreased adsorption of As(V) induced by *S. putrefaciens* CN-32 must result from direct bacteria-mineral surface interactions. *Shewanella* species have developed short rough lipopolysaccharides of high charge character to aid close adherence to mineral surfaces, such as Fe(III)-oxyhydroxides.[33] Living *S. putrefaciens* CN-32 cells can produce polysaccharides that are composed of core oligosaccharides and lipid A backbones without capsular polysaccharides.[33,34] The highly ionizable surface groups on the oligosaccharide backbones, for example, phosphate and carboxylate groups, may provide sites for particle attachment.[35,36] Using attenuated total reflectance Fourier transform infrared (ATR-FTIR) spectroscopy, we recently revealed As(V) desorption concurrent with attachment of *S. putrefaciens* CN-32 cells at the hematite (α-Fe_2O_3) surface at pH 7.0 via formation of inner-sphere complexes of surface Fe

with bacterial phosphate or carboxylate groups.[15] Furthermore, we showed inoculums of deactivated *S. putrefaciens* CN-32 cells to induce As(V) desorption from 0.2 g L^{-1} ferrihydrite and 0.2 and 2 g L^{-1} goethite under the same experimental conditions. In another related study, we found an increased As(V) reduction rate by *S. putrefaciens* CN-32 after addition of extracellular polymeric substances isolated from the same strain.[37] Therefore, the discrepancies between experimental and predicted As(V) reduction rates in the present study can most likely be explained by bacteria-mineral surface interactions that led to an increase in dissolved As(V) available for microbial reduction in solution.

Environmental Implications. In agreement with earlier reports for other bacterial strains, we showed that adsorption of As(V) to oxide mineral surfaces strongly reduces the rate of As(V) reduction by *S. putrefaciens* CN-32 under anoxic conditions. Our results demonstrate that microbial As(V) reduction in mineral-water systems, in which most of the total As is adsorbed to mineral surfaces, can proceed without significant reductive dissolution of Fe(III)-oxyhydroxides. Furthermore, we provided new evidence for surface interactions between *S. putrefaciens* CN-32 cells and mineral sorbents significantly enhancing desorption of As(V), thereby facilitating microbial As(V) reduction. Thus, the interplay between As(V) sorption at mineral surfaces and bacterially mediated As(V) desorption is likely critical with respect to the kinetics and extent of reductive As release, for example in aquifer sediments and rice paddy soils in young deltaic regions of South and Southeast Asia where elevated As concentrations in groundwater and soil pose serious health risks.

■ ASSOCIATED CONTENT

Supporting Information. Additional information on Langmuir isotherm fits (Table S1) and the negligible effect of lactate and acetate on As sorption (Figure S1); As(V) desorption and As(III) adsorption kinetics and modeling (Figures S2) including fitting parameters (Tables S2 and S3); dissolved As(V) and As(III) concentrations in the presence of ferrihydrite and boehmite during incubations (Figure S3); fitting parameters of microbial As(V) reduction kinetics in the presence of sorbents (Table S4), and competitive adsorption between As(III) and As(V) (Table S5). This material is available free of charge via the Internet at http://pubs.acs.org.

■ AUTHOR INFORMATION

Corresponding Author

*Phone: +41 44 632 88 19; e-mail: jenhow.huang@env.ethz.ch.

■ ACKNOWLEDGMENT

We gratefully acknowledge Kurt Barmettler (ETH) for technical support in the laboratory and Jakob Frommer (ETH) for help with N_2−BET measurements and kinetic modeling. This research was partially funded by a Marie Curie Intra-European Fellowship (Grant No. 039074) and an Ambizione grant from the Swiss National Science Foundation (Grant No. PZ00P2_122212) to the first author.

■ REFERENCES

(1) Smedley, P. L.; Kinniburgh, D. G. A review of the source, behaviour and distribution of arsenic in natural waters. *Appl. Geochem.* **2002**, *17*, 517–568.

(2) Smith, A. H.; Lingas, E. O.; Rahman, M. Contamination of drinking-water by arsenic in Bangladesh: a public health emergency. *Bull. W. H. O.* **2000**, *78*, 1093–1103.

(3) Horneman, A.; Van Geen, A.; Kent, D. V.; Mathe, P. E.; Zheng, Y.; Dhar, R. K.; O'Connell, S.; Hoque, M. A.; Aziz, Z.; Shamsudduha, M.; Seddique, A. A.; Ahmed, K. M. Decoupling of As and Fe release to Bangladesh groundwater under reducing conditions. Part 1: Evidence from sediment profiles. *Geochim. Cosmochim. Acta* **2004**, *68*, 3459–3473.

(4) Masscheleyn, P. H.; Delaune, R. D.; Patrick, W. H. Effect of redox potential and pH on arsenic speciation and solubility in a contaminated soil. *Environ. Sci. Technol.* **1991**, *25*, 1414–1419.

(5) Fendorf, S.; Kocar, B. D. Biogeochemical processes controlling the fate and transport of arsenic: Implications for South and Southeast Asia. *Adv. Agron.* **2009**, *104*, 137–164.

(6) Islam, F. S.; Gault, A. G.; Boothman, C.; Polya, D. A.; Charnock, J. M.; Chatterjee, D.; Lloyd, J. R. Role of metal-reducing bacteria in arsenic release from Bengal delta sediments. *Nature* **2004**, *430*, 68–71.

(7) Weber, F. A.; Hofacker, A. F.; Voegelin, A.; Kretzschmar, R. Temperature dependence and coupling of iron and arsenic reduction and release during flooding of a contaminated soil. *Environ. Sci. Technol.* **2010**, *44*, 116–122.

(8) Fendorf, S.; Michael, H. A.; van Geen, A. Spatial and temporal variations of groundwater arsenic in South and Southeast Asia. *Science* **2010**, *328*, 1123–1127.

(9) Harvey, C. F.; Swartz, C. H.; Badruzzaman, A. B. M.; Keon-Blute, N.; Yu, W.; Ali, M. A.; Jay, J.; Beckie, R.; Niedan, V.; Brabander, D.; Oates, P. M.; Ashfaque, K. N.; Islam, S.; Hemond, H. F.; Ahmed, M. F. Arsenic mobility and groundwater extraction in Bangladesh. *Science* **2002**, *298*, 1602–1606.

(10) Voegelin, A.; Weber, F. A.; Kretzschmar, R. Distribution and speciation of arsenic around roots in a contaminated riparian floodplain soil: Micro-XRF element mapping and EXAFS spectroscopy. *Geochim. Cosmochim. Acta* **2007**, *71*, 5804–5820.

(11) Frommer, J.; Voegelin, A.; Dittmar, J.; Marcus, M. A.; Kretzschmar, R. Biogeochemical processes and arsenic enrichment around rice roots in paddy soil: Results from micro-focused X-ray spectroscopy. *Eur. J. Soil Sci.* **2011**, *62*, 305–317.

(12) Manning, B. A.; Goldberg, S. Arsenic(III) and arsenic(V) adsorption on three California soils. *Soil Science* **1997**, *162*, 886–895.

(13) Stachowicz, M.; Hiemstra, T.; van Riemsdijk, W. H. Multicompetitive interaction of As(III) and As(V) oxyanions with Ca^{2+}, Mg^{2+}, PO_4^{3-}, and CO_3^{2-} ions on goethite. *J. Colloid Interface Sci.* **2008**, *320*, 400–414.

(14) Dixit, S.; Hering, J. G. Comparison of arsenic(V) and arsenic(III) sorption onto iron oxide minerals: Implications for arsenic mobility. *Environ. Sci. Technol.* **2003**, *37*, 4182–4189.

(15) Huang, J.-H.; Elzinga, E. J.; Brechbuehl, Y.; Voegelin, A.; Kretzschmar, R. Impacts of *Shewanella putrefaciens* strain CN-32 cells and extracellular polymeric substances on the sorption of As(V) and As(III) on Fe(III)-(hydr)oxides. *Environ. Sci. Technol.* **2011**, *45*, 2804–2810.

(16) Zobrist, J.; Dowdle, P. R.; Davis, J. A.; Oremland, R. S. Mobilization of arsenite by dissimilatory reduction of adsorbed arsenate. *Environ. Sci. Technol.* **2000**, *34*, 4747–4753.

(17) Campbell, K. M.; Malasarn, D.; Saltikov, C. W.; Newman, D. K.; Hering, J. G. Simultaneous microbial reduction of iron(III) and arsenic(V) in suspensions of hydrous ferric oxide. *Environ. Sci. Technol.* **2006**, *40*, 5950–5955.

(18) Tufano, K. J.; Reyes, C.; Saltikov, C. W.; Fendorf, S. Reductive processes controlling arsenic retention: revealing the relative importance of iron and arsenic reduction. *Environ. Sci. Technol.* **2008**, *42*, 8283–8289.

(19) Fakih, M.; Davranche, M.; Dia, A.; Nowack, B.; Morin, G.; Petitjean, P.; Chatellier, X.; Gruau, G. Environmental impact of As(V)-Fe oxyhydroxide reductive dissolution: An experimental insight. *Chem. Geol.* **2009**, *259*, 290–303.

(20) Jones, C. A.; Langner, H. W.; Anderson, K.; McDermott, T. R.; Inskeep, W. P. Rates of microbially mediated arsenate reduction and solubilization. *Soil Sci. Soc. Am. J.* **2000**, *64*, 600–608.

(21) Langner, H. W.; Inskeep, W. P. Microbial reduction of arsenate in the presence of ferrihydrite. *Environ. Sci. Technol.* **2000**, *34*, 3131–3136.
(22) Rochette, E. A.; Li, G. C.; Fendorf, S. E. Stability of arsenate minerals in soil under biotically generated reducing conditions. *Soil Sci. Soc. Am. J.* **1998**, *62*, 1530–1537.
(23) Cornell, R. M.; Schwertmann, U., *The Iron Oxides: Structure, Properties, Reactions, Ocurences and Uses*; Viley-VCH: Weinheim, 2003.
(24) Hofmann, A.; Pelletier, M.; Michot, L.; Stradner, A.; Schurtenberger, P.; Kretzschmar, R. Characterization of the pores in hydrous ferric oxide aggregates formed by freezing and thawing. *J. Colloid Interface Sci.* **2004**, *271*, 163–173.
(25) Mikutta, C.; Mikutta, R.; Bonneville, S.; Wagner, F.; Voegelin, A.; Christl, I.; Kretzschmar, R. Synthetic coprecipitates of exopolysaccharides and ferrihydrite. Part I: Characterization. *Geochim. Cosmochim. Acta* **2008**, *72*, 1111–1127.
(26) Huang, J. H.; Kretzschmar, R. Sequential extraction method for speciation of arsenate and arsenite in mineral soils. *Anal. Chem.* **2010**, *82*, 5534–5540.
(27) Yin, Y. J.; Allen, H. E.; Huang, C. P.; Sparks, D. L.; Sanders, P. F. Kinetics of mercury(II) adsorption and desorption on soil. *Environ. Sci. Technol.* **1997**, *31*, 496–503.
(28) Taillefert, M.; Beckler, J. S.; Carey, E.; Burns, J. L.; Fennessey, C. M.; DiChristina, T. J. Shewanella putrefaciens produces an Fe(III)-solubilizing organic ligand during anaerobic respiration on insoluble Fe(III) oxides. *J. Inorg. Biochem.* **2007**, *101*, 1760–1767.
(29) Lovley, D. R.; Holmes, D. E.; Nevin, K. P., Dissimilatory Fe(III) and Mn(IV) reduction. In *Advances in Microbial Physiology*; Academic Press Ltd: London, 2004; Vol. 49, pp 219−286.
(30) Gorby, Y. A.; Yanina, S.; McLean, J. S.; Rosso, K. M.; Moyles, D.; Dohnalkova, A.; Beveridge, T. J.; Chang, I. S.; Kim, B. H.; Kim, K. S.; Culley, D. E.; Reed, S. B.; Romine, M. F.; Saffarini, D. A.; Hill, E. A.; Shi, L.; Elias, D. A.; Kennedy, D. W.; Pinchuk, G.; Watanabe, K.; Ishii, S.; Logan, B.; Nealson, K. H.; Fredrickson, J. K. Electrically conductive bacterial nanowires produced by *Shewanella oneidensis* strain MR-1 and other microorganisms. *Proc. Natl. Acad. Sci. U. S. A.* **2006**, *103*, 11358–11363.
(31) Marsili, E.; Baron, D. B.; Shikhare, I. D.; Coursolle, D.; Gralnick, J. A.; Bond, D. R. *Shewanella* secretes flavins that mediate extracellular electron transfer. *Proc. Natl. Acad. Sci. U. S. A.* **2008**, *105*, 3968–3973.
(32) Amstaetter, K.; Borch, T.; Larese-Casanova, P.; Kappler, A. Redox transformation of arsenic by Fe(II)-activated goethite (alpha-FeOOH). *Environ. Sci. Technol.* **2010**, *44*, 102–108.
(33) Korenevsky, A. A.; Vinogradov, E.; Gorby, Y.; Beveridge, T. J. Characterization of the lipopolysaccharides and capsules of *Shewanella* spp. *Appl. Environ. Microbiol.* **2002**, *68*, 4653–4657.
(34) Nazarenko, E. L.; Komandrova, N. A.; Gorshkova, R. P.; Tomshich, S. V.; Zubkov, V. A.; Kilcoyne, M.; Savage, A. V. Structures of polysaccharides and oligosaccharides of some Gram-negative marine *Proteobacteria*. *Carbohydr. Res.* **2003**, *338*, 2449–2457.
(35) Parikh, S. J.; Chorover, J. ATR-FTIR study of lipopolysaccharides at mineral surfaces. *Colloid Surf. B* **2008**, *62*, 188–198.
(36) Parikh, S. J.; Chorover, J. ATR-FTIR spectroscopy reveals bond formation during bacterial adhesion to iron oxide. *Langmuir* **2006**, *22*, 8492–8500.
(37) Huang, J. H.; Melton, E. D.; Lazzaro, A.; Voegelin, A.; Zeyer, J.; Kretzschmar, R. Influence of competitive adsorption on kinetics of microbial arsenate reduction. *Geochim. Cosmochim. Acta* **2009**, *73*, A557–A557.